INSTITUTE OF PHYSICS PUBLISHING JOURNAL OF MICROMECHANICS AND MICROENGINEERING

J. Micromech. Microeng. **16** (2006) 1884–1890 doi:10.1088/0960-1317/16/9/018

Geometry and surface-assisted micro flow discretization*

Yu-Chuan Su[1] **and Liwei Lin**[2]

[1] Department of Engineering and System Science, National Tsing Hua University, Taiwan
[2] Department of Mechanical Engineering and Berkeley Sensor and Actuator Center, University of California, Berkeley, CA 94720-1740, USA

E-mail: ycsu@ess.nthu.edu.tw

Received 21 February 2006, in final form 10 July 2006
Published 4 August 2006
Online at stacks.iop.org/JMM/16/1884

Abstract

This paper presents a micro flow discretization system that autonomously digitizes continuous liquid flow into nanoliter segments. Powered by the interactions between liquid flow and micro-channels, the discretization process does not consume any electricity or require any external control. In the prototype demonstration, the discretizer is made of PDMS microfluidic channels with desired geometries and surface properties. Employing a novel self-aligned masking process followed by oxygen plasma treatment to pattern the three-dimensional channel surfaces, the areas exposed to plasma are converted from naturally hydrophobic into hydrophilic while the others covered by the mask remain hydrophobic. With the assistance of channel geometries and hydrophobic/hydrophilic surface patterns, continuous water flow has been split by interfacial forces into segments with controllable and pre-determined volumes from 15 to 35 nl. As such, this autonomous flow discretizer could serve a new class of metering and manipulation schemes for microfluidic applications including drug delivery and lab-on-a-chip.

(Some figures in this article are in colour only in the electronic version)

Introduction

Separation of liquid segments from a continuous source has been studied for decades. For example, a growing pendent drop may break away under gravity if its volume becomes too large such that the surface tension can no longer hold the entity [1–4]. However, when dimensions shrink, breakaway (or separation) becomes difficult because of the strong surface effects at the microscale. Micro droplets with characteristic dimensions ranging from several to hundreds of micrometers are highly desirable for a variety of applications, including inkjet printing, fuel injection, optical systems, IC cooling, combinatorial chemistry, bioassays and drug delivery [5, 6]. Previously, researchers had demonstrated micro droplet separations by using electro-wetting-on-dielectric (EWOD) schemes [7, 8], thermal bubble actuation [9, 10], PZT actuation [11, 12] and pressurized air [13]. Furthermore, continuous formation of liquid droplets has been demonstrated in systems containing two immiscible fluids [14–18]. To achieve droplet separation, the above approaches require sophisticated on-chip or external actuation schemes and/or adequate bi-liquid systems which may not be practical for remote sensing or implantable drug delivery applications. This work aims to develop an autonomous flow discretization system, which functions with the assistance of designed geometries and surface properties, operating without any external control or power supply.

Previously, we have demonstrated an implantable, water-powered, microfluidic delivery system with constant delivery rate for a long period of time [19]. Although continuous delivery can maintain fluidic concentration in a desired level for applications such as drug delivery to reduce adverse side effects, it is not always the best desirable delivery pattern. Many situations require, or would benefit from, an intermittent or pulsatile release of drugs (or fluids). The reasons vary, but mostly are related to the nature of physiological releases, which act in response to stimuli and allow for periods of restoration of certain bodily functions between consecutive

* A portion of this paper was presented at the 12th International Conference on Solid-State Sensors, Actuators, and Microsystems, June 2003, Boston, USA.

actions. For example, diabetic patients need insulin injections just several times per day. The release of insulin from a controlled delivery system should be induced only at moments when the body needs it, but does not necessarily last for a long period of time. On the other hand, long-term administration of many potent drugs, such as those used in cancer treatments, requires drug administration at certain time intervals to avoid poisoning of healthy tissues. Therefore, a discretization scheme, which facilitates the dosage metering and intermittent release of fluids, could be desirable for systems aiming to provide diversified delivery profiles.

To address this need, this work presents a new separation scheme, which is assisted by the interfacial interactions between fluids and micro-channels, to realize autonomous flow discretization for potential drug delivery and lab-on-a-chip applications. Three accomplishments have been achieved: (1) the guidelines for designing such kind of micro flow discretization systems, which are verified by both numerical simulations and experimental results, to facilitate the implementation; (2) a new surface patterning process employing self-aligned masks to generate hybrid hydrophobic/hydrophilic motifs and (3) an autonomous flow discretization system without external actuation or control. As such, this scheme could be applied to cooperate with micro bioassay or delivery systems to provide site-specific intermittent or pulsatile releases of fluidic samples, buffers or drugs.

Operation principle

When a droplet is separated from a continuous source, energy is supplied by the driving forces to create additional interfacial area between liquid and gas (or another liquid) while conserving the total liquid volume [20]. Furthermore, the driving forces must act against and also be strong enough to overcome the resistance caused by interfacial tensions. As mentioned in the previous section, there are a variety of sophisticated approaches that can discretize droplets from a continuous source. In this work, we aim to develop a simple approach for creating droplets in a pre-programmable manner by employing only interfacial tensions, which are controlled by factors including surface hydrophilicity (or hydrophobicity) and channel geometries. From an energy point of view, the system is first driven to an unstable state, which is the starting point of an autonomous path ended with discretization, and then spontaneously reaches the desired final state. Figure 1 shows the operation principle: (a) a micro flow discretization system with a hydrophilic microfluidic channel intersected by a designed hydrophobic region; (b) a steady liquid flow is driven into the hydrophobic region; (c) the flow reaches the entrance of a downstream micro-channel; (d) the narrow hydrophobic entrance prevents the flow from entering the downstream micro-channel and therefore (1) the liquid accumulates in the hydrophobic region; (2) the air enclosed on both sides is squeezed and pressurized and (3) the driving pressure increases to maintain the liquid flowing at a constant rate; (e) once the driving pressure overcomes the barrier built across the narrow hydrophobic entrance, the flow passes the entrance and is (1) squeezed by the compressed air; (2) sucked into the downstream hydrophilic channel and (3) expelled out of

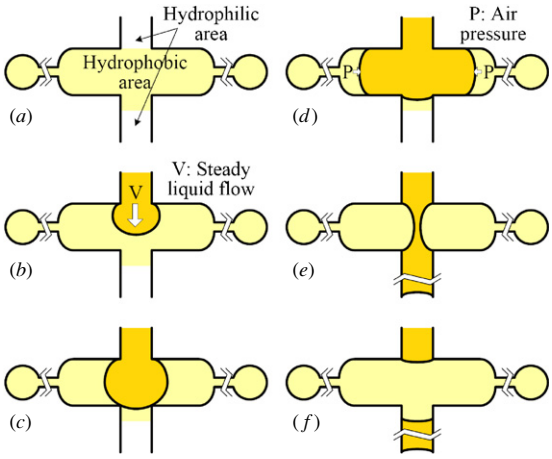

Figure 1. The microfluidic channel combining attractive and expulsive forces for flow discretization. (*a*) Geometry and surface properties, (*b*)–(*f*) splitting sequence.

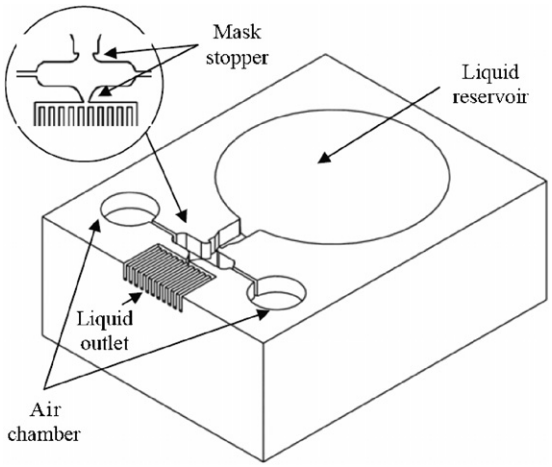

Figure 2. Schematic diagram of the flow discretizer.

the hydrophobic intersection to cause necking and breakaway at the junction and (f) process completes. After the first cycle, the downstream hydrophilic channel is filled with one liquid segment. Later in each of the following discretization cycle, one extra segment will be pushed and added into the downstream micro-channel.

This concept is straightforward and can be easily implemented on a microfluidic chip. Figure 2 shows the schematic design of the proof-of-concept prototype. The liquid reservoir supplies the incoming liquid and the air chambers are designed to store pressure to assist the separation process. On the other hand, two mask stoppers are employed to prevent the masking material, which is patterned in the liquid state and then solidified, from entering the designated hydrophilic regions. In operation, pressure barriers are built across the junction (as indicated in figure 3) and their magnitudes can be derived by the virtual work principles and approximated as [21]

$$\Delta P_1 = \frac{2\gamma}{w}\sin\theta_1, \tag{1}$$

$$\Delta P_2 = \frac{2\gamma}{w}\cos\theta_1, \tag{2}$$

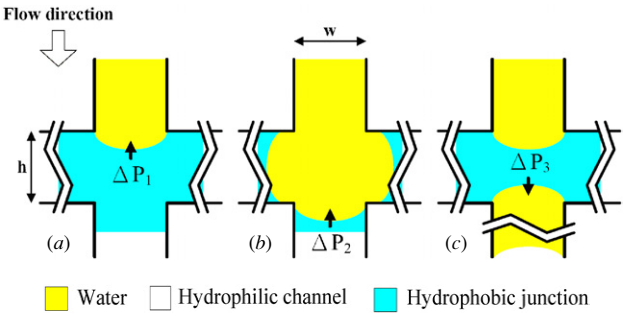

Figure 3. Pressure barriers built across the junction prevent water from (*a*) leaving the hydrophilic channel, (*b*) entering the narrow hydrophobic area and (*c*) staying in the hydrophobic area.

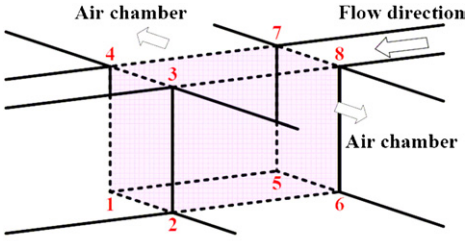

Facet 1: 1-5-6-2, Facet 2: 2-6-8-3
Facet 3: 3-8-7-4, Facet 4: 1-4-7-5

Figure 4. Schematic diagram of the geometry used in the simulation.

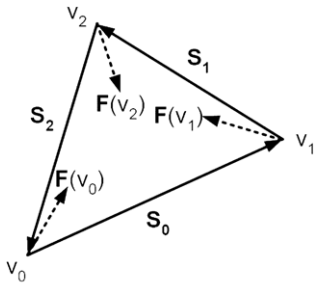

v: vertex, S: edge, F: force

Figure 5. Schematic diagram of a basic element used in the simulation program for surface energy minimization.

$$\Delta P_3 = \frac{2\gamma}{w}\sin\theta_1 + \frac{2\gamma}{w}\cos\theta_2, \tag{3}$$

where γ is the surface energy per unit area of the gas–liquid interface, w is the width of the microfluidic channel and θ_1 and θ_2 are the contact angles of the hydrophobic and hydrophilic surfaces, respectively. In figure 3(*a*), ΔP_1 is the required driving pressure to push water into the hydrophobic region. On the other hand, ΔP_2 (as indicated in figure 3(*b*)) affects the volume of water accumulated in the hydrophobic region before breakaway. A higher ΔP_2 typically results in more accumulation and therefore a larger volume of discretized segments. Furthermore, during the breakaway shown in figure 3(*c*), ΔP_3 assists the flow separation by pushing water away from the hydrophobic region and pulling it into the downstream hydrophilic micro-channel.

The most critical step in the splitting sequence is the final breakaway process shown in figures 1(*e*) and (*f*). The interfacial tensions built across the junction do not necessarily act appropriately to break the flow. Instead of breakaway, in many cases liquid flow tends to remain at necking states similar to that shown in figure 1(*e*). To identify the critical parameters relevant to the splitting of micro flow, Surface Evolver [22] is employed to simulate the equilibrium states of liquid surfaces under various interfacial interactions and geometrical constraints. As noted in figure 1(*e*), after liquid fills into the bottom hydrophilic channel, it is desired for the liquid remaining in the hydrophobic junction to reach an unstable necking state that spontaneously leads to the discretization of flow. From an energy point of view, in order to achieve spontaneous discretization, the overall surface energy should be monotonously decreasing from necking to the final separation states. In this work, we employ Surface Evolver to investigate the criteria that cause the monotonous energy decrease through the discretization process. First of all, an initial shape of the liquid surfaces in the junction is applied as shown in figure 4. In this case, 8 vertices (indicated with numbers from 1 to 8), 12 edges and 4 facets (bounded by the edges connecting vertices 2-6-8-3, 3-8-7-4, 1-4-7-5 and 1-5-6-2) are defined in the model. The overall surface energy is the sum of the surface energy corresponding to its two free surfaces (facets 2 and 4) and two contact surfaces with the microfluidic channel (facets 1 and 3) as indicated in figure 4. The eight vertices and eight edges connecting vertices 1-2, 2-3, 3-4, 4-1, 5-6, 6-7, 7-8 and 8-5 are fixed while the other four edges and four facets are allowed to deform during the evolving process. Among these deformable edges, the ones connecting vertices 1-5 and 2-6 are constrained at the bottom plane to consider the effect of gravity. Afterward, surface energy functions associated with these three-dimensional interfaces are specified. Here we assume that gravity and the attractive/expulsive forces acting on the liquid will lower down facet 3 and alter it into a liquid–gas interface. Therefore, facets 2, 3 and 4 are modeled as liquid–gas interfaces and facet 1 is modeled as a liquid–solid interface with a contact angle of 100°. Surface Evolver then meshes the surfaces into small triangular elements and modifies these elements, subject to the given constraints, to minimize the overall surface energy. Considering an individual triangular element, as shown in figure 5, its surface energy can be expressed as [22]

$$E = \frac{T}{2}\|\vec{s}_0 \times \vec{s}_1\|, \tag{4}$$

where T is the surface energy per unit area and $\vec{s}_0$ and $\vec{s}_1$ are two edge vectors of the element. Since the derivative of strain energy with respect to displacement equals the corresponding force, the surface force induced at one specific vertex can be expressed as

$$\vec{F}(v_0) = \frac{T}{2}\frac{\vec{s}_1 \times (\vec{s}_0 \times \vec{s}_1)}{\|\vec{s}_0 \times \vec{s}_1\|}. \tag{5}$$

By moving each vertex along the net force induced at it, the overall surface energy will eventually reach its minimum and the equilibrium state can be found.

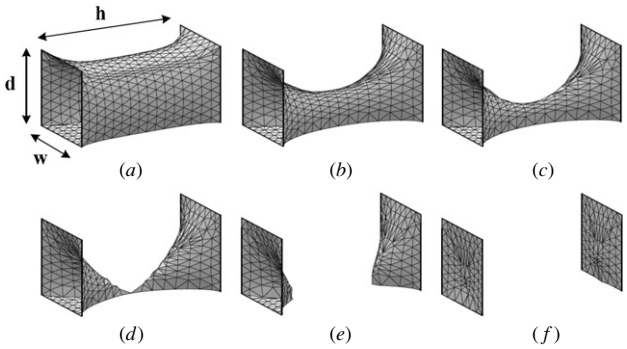

Figure 6. A successful breakaway sequence simulated by Surface Evolver.

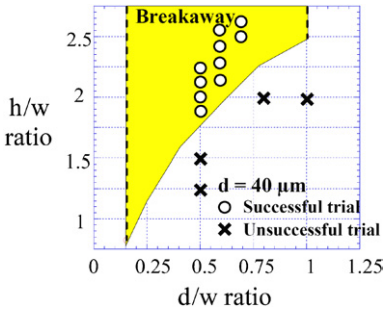

Figure 7. Simulation results by Surface Evolver (breakaway will spontaneously occur in the filled areas).

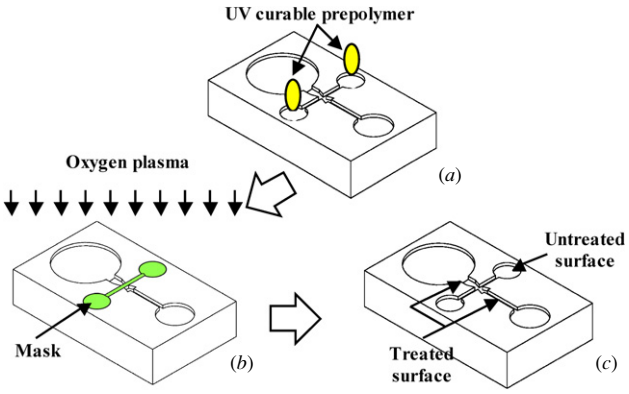

Figure 8. The surface patterning process: (*a*) selective casting of a liquid pre-polymer (*b*) oxygen plasma surface treatment and (*c*) final result.

The depth (d) and width (w) of the hydrophilic channel and the length (h) of the hydrophobic junction are identified as the critical parameters and numerical simulations are performed to characterize the criteria of spontaneous breakaway. Figure 6 shows an evolving sequence from the simulations that predicts a successful breakaway. Typically, the junction length (h) has to be long enough to drive the total surface energy to an unstable necking state that breakaway will occur afterward spontaneously to minimize the overall surface energy. Figure 7 shows the simulation results, which will be employed as design guidelines, with filled areas (including data from the prototype design parameters) indicating breakaway will autonomously occur.

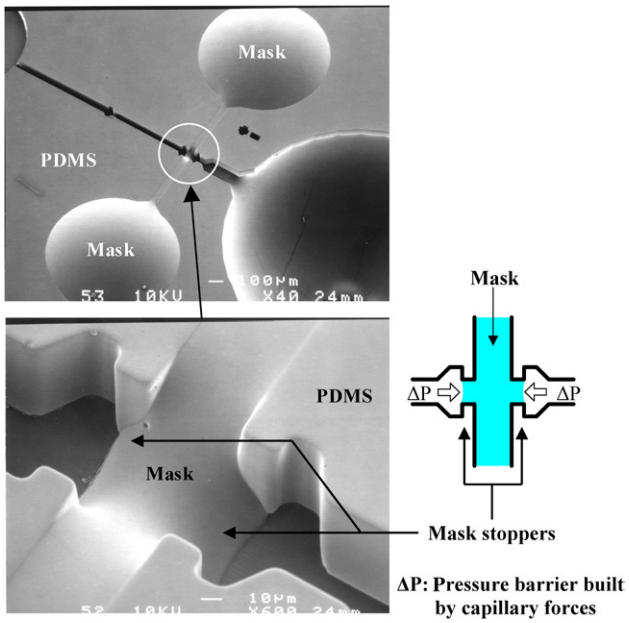

Figure 9. SEM micrographs of the micro-channel partially filled and covered by self-aligned mask and a close view near the junction.

The fabrication process

Polydimethylsiloxane (PDMS) is used to fabricate the device for prototype demonstration. A layer of 40 μm thick negative photoresist (MicroChem SU-8 100) is spin coated and patterned on the top of a clean silicon wafer to create a mold for duplicating microfluidic components in the following polymer casting process. After the SU-8 mold is fully cured, it is placed in a desiccator under vacuum for 2 h with a vial containing a few drops of tridecafluoro-1,1,2,2-tetrahydrooctyl-1-trichlorosilane to silanize the surfaces [23]. Silanization of the mold facilitates the removal of polymeric replicas after casting. A mixture of 10:1 PDMS pre-polymer and curing agent (Dow-Corning Sylgard 184) is stirred thoroughly and then degassed under vacuum. The pre-polymer and curing agent mixture are then poured onto the mold, degassed and cured for 2 h at 85 °C. After thoroughly cured, this PDMS replica is peeled off from the mold.

The major challenge in fabricating the flow discretizer is the patterning of hydrophobic and hydrophilic regions inside the PDMS microfluidic channel. Because of the depth and the vertical sidewalls of the microfluidic channel, conventional two-dimensional masking processes are inappropriate for patterning the three-dimensional channel surfaces. Based on the knowledge that hydrophobic PDMS surfaces can be converted to hydrophilic using oxygen plasma treatment [23], a new self-aligned masking process is developed and UV-curable adhesives are chosen as the masking materials. The patterning process is shown in figure 8. First, a UV-curable pre-polymer (Norland Optical Adhesive 83H), which tends to wet PDMS surfaces, is poured into the air chambers (shown in figure 2) to fill up the designate hydrophobic region. The flow of the pre-polymer is blocked by the specially designed stoppers as illustrated in figure 9, where pressure barriers are built by capillary forces to prevent the pre-polymer from moving forward. It is observed that an abrupt 90° angle

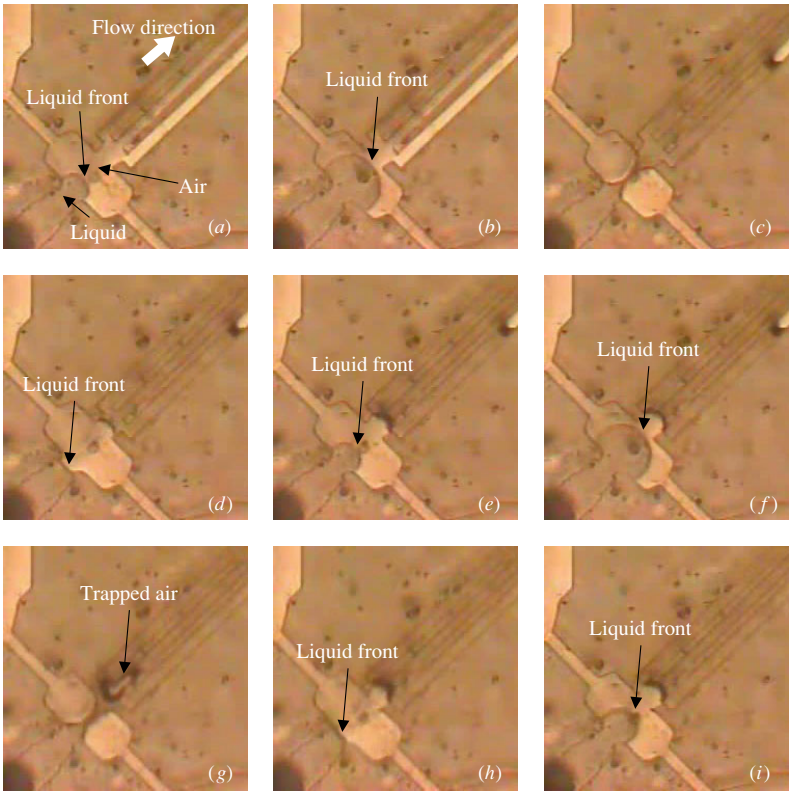

Figure 10. A series of flow discretization sequences: (*a*), (*b*) liquid is propelled into the hydrophobic area; (*c*) liquid is attracted and expelled into the hydrophilic area; (*d*) flow is split and the first cycle ends; (*e*)–(*h*) flow is split again in the second cycle and (*i*) the third cycle starts.

cutting into the channel sidewall as shown is adequate for this purpose. Once the designate hydrophobic region is completely covered with the liquid pre-polymer, UV light is applied to strengthen and solidify the polymeric mask. The solidified mask is used to protect the designate areas during the surface treatment process, which uses oxygen plasma to modify the surface as shown in figure 8(*b*). After the treatment, desired hydrophobic/hydrophilic patterns are generated and the mask is forcefully peeled off from the channel. At the end, a hydrophobic PDMS cover is added to complete the fabrication process.

Experimental result

Figure 10 shows a series of observed flow discretization sequences that concurs with the operation principle illustrated in figure 1. Before water is introduced, the microfluidic channel is empty and has a brighter color. With no external pressure applied, water fills the hydrophilic part of the channel spontaneously due to surface tension and stops in front of the hydrophobic junction area. In the demonstration, water is driven at a constant flow rate of 4 nl min^{-1} by a syringe pump. Once water is driven into the junction, the color of the filled area becomes darker and the interface between water and air can be clearly observed under a microscope. With the dimensions employed in our prototype demonstration (including widths ranging from 60 μm to 80 μm and lengths ranging from 150 μm to 180μm), the accumulation step takes roughly 4–8 min for the water flow to finally reach the other end of the junction area. After that, the breakaway process

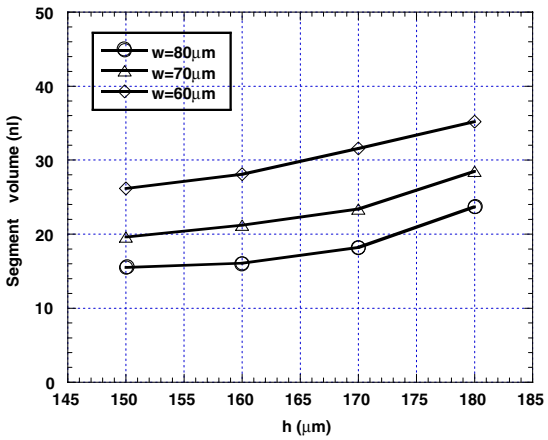

Figure 11. Measured segment volume with respect to geometry of the flow discretizer.

takes less than 10 s to complete. The dimensions of the microfluidic channel are specified following the rules acquired from the simulation results in figure 7 to ensure successful breakaway. Totally, we have 12 different channel designs (some indicated as circles in figure 7) and all of them result in successful discretization. On the other hand, designs with dimensions violating the rules are also tested and it is observed that discretization fails when operated in these channel designs (some indicated as crosses in the figure). Figure 11 shows the measured segment sizes of 15–35 nl affected by dimensions of the 12 different channel designs. Generally speaking, wider

channels (with larger w) will result in discretized segments with smaller volumes and longer junctions (with larger h) will create segments with larger volumes.

Discussion

The simulation results shown in figure 7 indicate the lower bounds of h/w ratio that cause spontaneous breakaway when d/w ratio varies. For example, with $d = 40$ μm and $w = 80$ μm ($d/w = 0.5$), h needs to be longer than 140 μm ($h/w > 1.25$) to promote separation. If w is reduced to 40 μm ($d/w = 1$), a junction length longer than 100 μm ($h/w > 2.5$) will be enough to facilitate breakaway. In this work, we study only the cases with $d = 40$ μm and d/w ratios ranging from 0.15 to 1 because of manufacturing convenience. Figure 7 predicts that lower d/w and higher h/w ratios, which correspond to wider channels and longer junctions, will facilitate discretization. The experimental results indicated in figure 7, in which all the ten designs with d/w and h/w ratios located in the filled area result in successful breakaway and all the four designs located outside fail in our experiments, verify the prediction. In case a depth other than 40 μm or a d/w ratio located outside the range between 0.15 and 1 is employed, similar simulation can be performed to acquire the design guidelines.

According to the experimental results shown in figure 11, smaller channel widths (w) and larger junction lengths (h) tend to produce discrete fluidic segments with larger volumes. Basically, the volume of a generated fluidic segment is a portion of the volume of fluid accumulated in the junction area before breakaway. Because the fluid is pushed by a syringe pump, which induces a constant flow rate while the driving pressure varies, accumulation continues until the driving pressure is eventually raised above the pressure barrier set by the narrow hydrophobic entrance as illustrated in figure 3(b). From equation (2), smaller channel widths tend to build higher pressure barriers across the entrance, and therefore more fluid accumulates in the junction area before bursting into the downstream micro-channel. In addition, unintentional accumulation caused by the deformation of plastic tubes and the PDMS chip, which contributes a fraction of the segment volume, is also observed. On the other hand, because there is more space in a longer junction to store fluid before breakaway, it also tends to generate discrete fluidic segments with larger volumes. Depending on the requirements for specific applications, sets of geometrical parameters (h, w and d) can be determined and employed to generate segments with desired volumes.

In our design, the discretization of a continuous flow into separated segments is facilitated by the designed hydrophilic/hydrophobic patterns inside the PDMS micro-channels. In the prototype demonstration, these patterns are generated by the self-aligned masking process and following oxygen plasma treatment, which selectively modify the wettability of PDMS surfaces. However, the plasma-oxidized PDMS surfaces are known to gradually recover its hydrophobicity after the treatment [24]. In a few hours or days, the migration of short PDMS chains from bulk to the surface converts the treated hydrophilic surfaces back to hydrophobic. The rapid loss of hydrophilicity will consequently cause the failure of our discretization system and make it unreliable for long-term applications. To generate surface patterns with better long-term stability, coating with physically and chemically stable polymers could be a potential solution [25, 26]. When these alternative surface modification schemes are employed, our self-aligned masking process could cooperate with them to provide the required selectivity in surface patterning.

One potential application for the demonstrated flow discretizer is to provide intermittent release of drugs for therapeutic purposes. When a flow discretizer to provide pulsatile delivery profile is employed, air in the junction area serves as an excellent diffusion barrier because it blocks the diffusion pathway in most time and the only period diffusion occurs is during the breakaway period that is in the range of seconds based on experimental observations. For example, continuous drug delivery may result in contamination by diffusion and the diffusion rate through the continuous delivery channel can be simplified as follows [19]:

$$Q = DA\frac{\Delta C}{L}, \tag{6}$$

where D is the diffusivity through the liquid in the channel, A is the cross-sectional area of the channel, ΔC is the concentration difference across the channel and L is the length of the channel. Generally, the channel needs to have small cross section and significant length to reduce the diffusion rate into and out of the delivery channel. Considering a case of a common drug formulation (with $D = 3 \times 10^{-10}$ m^2 s^{-1} and $\Delta C = 0.4$ mg μl^{-1}) diffusing through a micro-channel with $A = 50 \times 40$ μm^2 and $L = 100$ μm, the diffusion rate is 2.4×10^{-6} mg s^{-1} and the total diffusion mass in 10 s is 2.4×10^{-5} mg, which is only about 0.15% of one digitized fluid segment as observed in experiments. For practical applications, this flow discretizer can be integrated with a constant-rate delivery system to provide site-specific intermittent or pulsatile release of drugs.

Conclusion

A micro flow discretizer that autonomously digitizes continuous liquid flow into nanoliter segments is demonstrated. The prototype discretizer is made of PDMS with simulation-verified geometries and surface properties for flow separation. To define the desired surface patterns on the three-dimensional PDMS channels, a novel self-aligned masking process followed by oxygen plasma treatment is developed to selectively modify the surface properties. The operation principle of the flow discretization is based on the design of geometries and surface properties to facilitate the spontaneous separation of flow at the microscale. With the assistance of channel geometry and hydrophobic/hydrophilic surface patterns, successful discretization of continuous water flow into segments with volumes from 15 to 35 nl has been demonstrated. Future work may include the integration with a pressure source, such as the previously developed osmotic pumping device, to build a complete system capable of delivering fluids autonomously. As such, this autonomous flow discretizer represents a new class of metering and manipulation scheme for applications such as lab-on-a-chip and drug delivery systems.

Acknowledgments

The authors would like to thank Alza, Dow, DuPont and Kraton for providing testing samples. These devices are fabricated in the UC-Berkeley Microfabrication Laboratory (silicon and SU-8 molds) and Microsystem Laboratory (plastic parts). This work is supported in part by a DARPA/DSO/BioFlips grant F30602-00-2-0566.

References

[1] Rayleigh W S 1878 On the instability of jets *Proc. Lond. Math. Soc.* **10** 4–13
[2] Shi X D, Brenner M P and Nagel S R 1994 A cascade of structure in a drop falling from a faucet *Science* **265** 219–22
[3] Doshi P, Cohen I, Zhang W W, Siegel M, Howell P, Basaran O A and Nagel S R 2003 Persistence of memory in drop breakup: the breakdown of universality *Science* **302** 1185–8
[4] Middleman S 1995 *Modeling Axisymmetric Flows: Dynamics of Films, Jets, and Drops* (San Diego: Academic)
[5] Lee E R 2003 *Microdrop Generation* (Boca Raton: CRC Press)
[6] Nguyen N T and Wereley S T 2002 *Fundamentals and Applications of Microfluidic* (Boston: Artech House Publishers)
[7] Pollack M G, Shenderov A D and Fair R B 2002 Electrowetting-based actuation of droplets for integrated microfluidics *Lab Chip* **2** 96–101
[8] Cho S K, Moon H and Kim C J 2003 Creating, transporting, cutting, and merging liquid droplets by electrowetting-based actuation for digital microfluidic circuits *J. Microelectromech. Syst.* **12** 70–80
[9] Nielsen N J 1985 History of thinkjet printhead development *Hewlett-Packard J.* **36** 4–20
[10] Tseng F G, Kim C J and Ho C M 2002 A high-resolution high-frequency monolithic top-shooting microinjector free of satellite drops *J. Microelectromech. Syst.* **11** 427–47
[11] de Heij B, Steinert C, Sandmaier H and Zengerle R 2003 A tunable and highly-parallel picoliter dispenser based on direct liquid displacement *Sensors Actuators* A **103** 88–92
[12] Fuller S B, Wilhelm E J and Jacobson J M 2002 Ink-jet printed nanoparticle microelectro-mechanical systems *J. Microelectromech. Syst.* **11** 54–60
[13] Handique K, Burke D T, Mastrangelo C H and Burns M A 2001 On-chip thermopneumatic pressure for discrete drop pumping *Anal. Chem.* **73** 1831–38
[14] Thorsen T, Roberts R W, Arnold F H and Quake S R 2001 Dynamic pattern formation in a vesicle-generating microfluidic device *Phys. Rev. Lett.* **86** 4163–6
[15] Nisisako T, Torii T and Higuchi T 2002 Droplet formation in a microchannel network *Lab Chip* **2** 24–6
[16] Link D R, Anna S L, Weitz D A and Stone H A 2004 Geometrically mediated breakup of drops in microfluidic devices *Phys. Rev. Lett.* **92** 054503
[17] Tan Y C, Fisher J S, Lee A I, Cristini V and Lee A P 2004 Design of microfluidic channel geometries for the control of droplet volume, chemical concentration, and sorting *Lab Chip* **4** 292–8
[18] Tice J D, Song H, Lyon A D and Ismagilov R F 2003 Formation of droplets and mixing in multiphase microfludics at low values of the Reynolds and the capillary numbers *Langmuir* **19** 9127–33
[19] Su Y C and Lin L 2004 A water-powered micro drug delivery system *J. Microelectromech. Syst.* **13** 75–82
[20] Adamson A W and Gast A P 1997 *Physical Chemistry of Surfaces* (New York: Wiley)
[21] Man P F, Mastrangelo C H, Burns M A and Burke D T 1998 Microfabricated capillarity-driven stop valve and sample injector *Proc. IEEE Workshop on Micro Electro Mechanical Systems (Heidelberg)* pp 45–50
[22] Brakke K A 2002 *Surface Evolver Manual* (Selinsgrove: Susquehanna University)
[23] Duffy D C, Mcdonald J C, Schueller O J A and Whitesides G M 1998 Rapid prototyping of microfluidic systems in poly(dimethylsiloxane) *Anal. Chem.* **70** 4974–84
[24] Makamba H, Kim J H, Lim K, Park N and Hahn J H 2003 Surface modification of poly(dimethyl-siloxane) microchannels *Electrophoresis* **24** 3607–19
[25] Lahann J, Balcells M, Lu H, Rodon T, Jensen K F and Langer R 2003 Reactive polymer coatings: a first step toward surface engineering of microfluidic devices *Anal. Chem.* **75** 2117–22
[26] Makamba H, Hsieh Y Y, Sung W C and Chen S H 2006 Stable permanently hydrophilic protein-resistant thin-film coatings on poly(dimethylsiloxane) substrates by electrostatic self-assembly and chemical cross-linking *Anal. Chem.* **77** 3971–8